J. Microbiol. Biotechnol. (2007), **17**(11), 1789–1796

JOURNAL OF MICROBIOLOGY AND BIOTECHNOLOGY

Molecular Orbital Theory on Cellulolytic Reactivity Between *p*NP-Cellooligosccharides and β-Glucosidase from *Cellulomonas uda* CS1-1

YOON, MIN-HO[1], YUN-KYU NAM[2], WOO-YOUNG CHOI[1]*, AND NACK-DO SUNG[1]

[1]*Division of Applied Biology and Chemistry, College of Agriculture and Life Sciences, Chungnam National University, Daejeon 305-764, Korea*
[2]*Department of Bioenvironment, Agricultural Research & Extension Services of Chungcheongnam-Do Province, 340-861, Korea*

Received: March 18, 2007 Accepted: June 27, 2007

Abstract A β-glucosidase with the molecular mass of 160,000 Da was purified to homogeneity from cell extract of a cellulolytic bacterium, *Cellulomonas uda* CS1-1. The kinetic parameters (K_m and V_{max}) of the enzyme were determined with *p*NP-cellooligosccharides (DP 1-5) and cellobiose. The molecular orbital theoretical studies on the cellulolytic reactivity between the *p*NP-cellooligosaccharides as substrate (S) molecules and the purified β-glucosidase (E) were conducted by applying the frontier molecular orbital (FMO) interaction theory. The results of the FMO interaction between E and S molecules verified that the first stage of the reaction was induced by exocyclic cleavage, which occurred in an electrophilic reaction based on a strong charge-controlled reaction between the highest occupied molecular orbital (HOMO) energy of the S molecule and the lowest occupied molecular orbital (LUMO) energy of the hydronium ion (H_3O^+), more than endocyclic cleavage, whereas a nucleophilic substitution reaction was induced by an orbital-controlled reaction between the LUMO energy of the oxonium ion (SH^+) protonated to the S molecule and the HOMO energy of the H_2O_2 molecule. A hypothetic reaction route was proposed with the experimental results in which the enzymatic acid-catalyst hydrolysis reaction of E and S molecules would be progressed *via* SN_1 and SN_2 reactions. In addition, the quantitative structure-activity relationships (QSARs) between these kinetic parameters showed that K_m has a significant correlation with hydrophobicity (logP), and specific activity has with dipole moment, respectively.

Keywords: Cellulolytic reactivity, *Cellulomonas uda* CS1-1, β-glucosidase, *p*NP-β-cellooligosaccharides, MO theory

β-Glucosidases are widely distributed in animals, plants, fungi, and bacteria. They hydrolyze cellobiose to glucose in the final step of cellulose degradation. Because the cellobiose acts as an inhibitor of other cellulase enzymes such as endo-β-1,4-glucanase and exo-β-1,4-glucanase [14], they play important roles to remove the inhibitory effect of cellulolytic enzymes.

Enzyme reactions are biologically catalyzed by a variety of ionizable groups functioning as electrophiles, nuclephiles, or general acid/base catalysts [3, 15, 16]. As a result, the pka values of one or a few key ionizable groups within its active-site cleft are employed as the factors to define the experimental and theoretical functions of these catalytically essential groups or to establish the pathway of a given enzyme reaction. For example, a comparison of active sites of endoglycosidases reveals a striking correlation with these pka values, in that the residue hydrogen bonded to the general acid/base catalyst is asparagine in an alkaline pH circumstance, whereas it is aspartic acid in those with a more acidic pH optimum [29].

The application of quantitative structure-activity relationships (QSARs) analyses on enzymatic reactions with substrate (S) molecules have provided another theoretic basis for understanding the enzymatic reactivities between enzyme (E) and S molecules [9]. The QSAR has also rendered rapid progress on the knowledge of protein structures available for synthesizing and designing more effective new enzymes [13]. The studies on QSAR analyses of the compounds relevant to the enzymatic reaction were initiated with fibrinolytic activity by Hansch and his coworkers [11, 16], in which they identified that the hydrophobicity (logP) of carbonic acids has a positive correlation with the fibrinolytic ability. When the E-S complexes are being formed in the hydrolysis reaction of glycosidic bond combined with phenoxy group substituted to glucose by emulsin (β-glucosidase), the hydrophobic interaction increases and desorption of the phenoxy moiety from the surface of enzymes in a step of the catalytic reaction is hindered by the increased hydrophobic effect [10].

A number of studies on hydrolysis reactions of the glycosidic bond caused by certain enzymes have been

*Corresponding author
Phone: 82-42-821-6733; Fax: 82-42-823-9241;
E-mail: wychoi@cnu.ac.kr

conducted until now [4, 5, 10, 20, 25, 29]. However, studies on molecular orbital (MO) theory and QSARs relevant to the reactivity of enzymatic hydrolysis attributed by β-glucosidase for β-1,4-glycosidic linkages within cellooligosaccharides are rare.

In this work, the physical and kinetic characterizations of β-glucosidase purified from *Cellulomonas uda* CS1-1 are reported. Furthermore, we describe the results on the enzymatic hydrolysis reactivity between the β-1,4-glucosidic bond in *p*NP-β-cellooligosaccharides (DP 1-5) and the β-glucosidase enzyme by means of the application of frontier molecular orbital (FMO) interaction theory [8] and QSAR methodology [18] with the obtained kinetic parameters.

MATERIALS AND METHODS

Organism and Culture Condition

Cellulomonas uda CS1-1 (KCTC 1371) was grown on Dubos' salt [31] solution supplemented with 0.05% yeast extract and 10 mM glucose as the carbon source to purify β-glucosidase from cell extract. The cultivation was carried out in a Quickfit FV5L fermenter for 2 days at 30°C.

Purification of β-Glucosidase

The purification of a β-glucosidase from cell extract of *Cellulomonas uda* CS1-1 was performed by means of successive chromatography on Ultro-gel Ac34, DEAE-Sephadex A-50, and hydroxyapatite. A 5-ml aliquot of the enzyme solution, which was collected from cell extract by 30–80% ammonium sulfate saturation, was applied to a column (1.8×100 cm; bed volume, 220 ml) of Ultro-gel Ac34. The elution was carried out with 20 mM phosphate buffer, pH 6.8, at a flow rate of 15 ml h^{-1}. A 5-ml aliquot of active fractions from the preceding step was applied to a column (2.3×30 cm; bed volume, 130 ml) of DEAE-Sephadex A-50 with exchange capacity of 3.5±0.5 milliequivalent per gram, which was equilibrated with 50 mM Tris-HCl buffer, pH 7.5. Elution of the column was performed with a linear salt gradient of 250 ml of 50 mM Tris-HCl buffer, pH 7.5, and 250 ml of 0.5 M sodium chloride in the same buffer. The flow rate was adjusted to 15 ml h^{-1}. A 5-ml aliquot of the enzyme from the preceding step was applied to a column (1.8×25 cm; bed volume, 50 ml) of hydroxyapatite, which was equilibrated with 40 mM phosphate buffer, pH 6.8. Elution of the column was performed with 50 ml of 40 mM phosphate buffer, pH 6.8, and 50 ml of 0.4 M phosphate buffer by a linear gradient and the flow rate was adjusted to 15 ml h^{-1}.

Assay of β-Glucosidase Activity

β-Glucosidase activity was determined with *p*-nitrophenyl-β-D-glucopyranoside (*p*NPG) as the substrate. Enzyme solution (1 ml) was added to the preincubated solution at 40°C for 10 min, which contained 1.5 ml of McIlvaine buffer, pH 6.4, and 0.5 ml of 5 mM *p*NPG. After incubation for 20 min at 40°C, the enzyme activity was stopped by adding 2 ml of 1 M sodium carbonate. The absorbance of the yellow color that developed from the *p*-nitrophenolate anion was monitered at 400 nm (ε=18.3 mM^{-1} cm^{-1}) and compared with a standard curve constructed using *p*-nitrophenol (*p*NP). The enzyme activity toward cellobiose was assayed by the glucose oxidase/peroxidase method [24].

Estimation of Protein and Molecular Mass

Protein content was determined by the method of Lowry *et al.* [21] with bovine serum albumin as a standard. The enzyme proteins of each purification step were identified by native- or SDS-PAGE using a vertical slab gel (Model AE-6640, Atto Co., Japan) at 10% of acrylamide concentration. The molecular mass was determined by SDS-PAGE using the method of Laemmli [19].

Hydrolysis Products of *p*NP-Cellooligosaccharides

To estimate the reaction products of β-glucosidase obtained during degradation of *p*-nitrophenyl-cellooligosaccharides (*p*NPG_n, n=2–5, Seikagaku Kogyo Co., Japan) as substrates, the chromophoric hydrolysis products, *p*NPG_1, *p*NPG_2, *p*NPG_3, and *p*NPG_4 released from *p*NPG_n, were separated by HPLC on a Develosil ODS-5 column (150×4.5 mm ID, Nomura Chemical Co., Japan). Two hundred μl of reaction mixtures that contained 2 units of enzyme and 0.2 mM of substrates in a 50 mM McIlvain buffer, pH 6.5, were incubated at 40°C with time interval ranging from 0.1 to 12 h, and then the reaction was stopped by placing the tube in a boiling water bath for 15 min. Aliquots (10 μl) of reaction mixture were applied to the column and the reaction products were eluted by a linear gradient of 0.3% butanol in 10 mM McIlvain buffer (A), pH 3.8, and 0.7% butanol in the same buffer (B) at 1.5 ml min^{-1} and monitored spectrophotometrically at 300 nm.

Kinetic Constants

The hydrolysis products of *p*NPGn (n=2–5) with β-glucosidase from *C. uda* CS1-1 were measured using HPLC analysis. Michaelis constants (K_m; mM), maximum velocities (V_{max}; mM min^{-1} mg^{-1} protein), and specific activities (SA; mM min^{-1} mg^{-1}) of the enzyme were determined by calculating the molar ratios of the reaction products. The values of *p*NPG and cellobiose were estimated by the assay conditions described in Methods.

Physicochemical Parameters and MO Functions

The most stable conformers of three-dimensional structure were determined by minimizing the *p*-nitrophenyl (*p*NP) group substituted molecules to the anomeric C_1-atom in β-

Table 1. Summary of purification steps for β-glucosidase from *C. uda* CS1-1.

Purification step	Total protein (mg)	β-Glucosidase activity*			
		Total activity (units)	Specific activity (units/mg)	Yield (%)	Purification factor (fold)
Crude enzyme	410	3,900	9.6	100	1.0
Ammonium sulfate (0.3–0.8 satn.)	286	3,620	16.2	93	1.7
Ultro-gel Ac 34 AF-I (Fr. Nos. 15–28)	150	3,250	19.6	83	2.0
DEAE A-50 D-I (Fr. Nos. 25–36)	30	2,100	70	54	7.3
Hydroxyapatite H-II (Fr. Nos. 15–28)	10	1,640	164	42	17.0

*β-Glucosidase activity was determined with *p*-nitrophenyl-β-D-glucopyranoside as the substrate at 400 nm.

cellooligosaccharides [β-(Glc)$_1$–β-(Glc)$_5$] linkage to the 1,4-β-glycosidic bond as substrate (S). The 21 physicochemical parameters of the most stable conformers, which are the STERIMOL parameters (Å) (L, B$_1$–B$_5$)[8], hydrophobicity (logP) [28], dipole moment (DM), lipole moment (LM), molecular volume (Å^3), molar refractivity (MR; cm^3/mol), molecular surface area (Å^2), and polar surface area (Å^2) [10] *etc.*, were calculated and then the 2D-QSAR models for the enzymatic hydrolysis were derived using the TSAR program (Ver. 3.3) [1]. And also the values of MO function such as HOMO (highest occupied molecular orbital) energy (e.v.), LUMO (lowest occupied molecular orbital) energy (e.v.), net charge, and atomic orbital (AO) coefficient were also calculated using the AMI method [7], which is a semiempirical molecular orbital theory in MOPAC [27].

Results and Discussion

Purification of β-Glucosidase

A β-glucosidase from the cell extract of *Cellulomonas uda* CS1-1 was purified to homogeneity by means of successive chromatography on Ultro-gel Ac34, DEAE-Sephadex A-50, and hydroxyapatite. As summarized in Table 1, the specific activity and purification factor of the purified enzyme were 164 units/mg and 17 folds as *p*NPG activity, respectively, and the molecular mass was identified as 160,000 Da by SDS-PAGE (Fig. 3A).

Kinetics of the Purified β-Glucosidase

The kinetic studies of the purified β-glucosidase were performed with various substrates. When the K_m values for *p*NPG and cellobiose were estimated using the Michaelis-Menten equation [23], typical Michaelis-Menten kinetics were observed by plotting the rate of enzyme activity against *p*NPG at the concentration of 125 μM–10 mM, and cellobiose at 5 mM–8 mM (data not shown). In addition, by the Lineweaver-burk plots, K_m values for *p*NPG and cellobiose were 1.33 and 0.24 mM, and V_{max} were 65.6 and 6.0 mM min^{-1} mg^{-1} protein (Table 2), respectively. Although the affinity on *p*NPG was lower than cellobiose, the value of V_{max} was higher (than that). This means that the enzyme has high turnover for the *p*NPG substituted with the *p*-nitrophenyl group rather than cellobiose as substrate. In the case of kinetic parameters for *p*NP-cellooligosaccharides (DP 2-5), the K_m values for *p*NPG$_2$, *p*NPG$_3$, *p*NPG$_4$, and *p*NPG$_5$ were calculated as 1.60, 0.32, 0.021, and 0.011 mM, and V_{max} values for each substrate were 0.14, 0.25, 0.63, and 2.63 mM min^{-1} mg^{-1} protein, respectively (Table 2). The hydrolysis rate of *p*NPG$_5$ appeared to exceed nearly four-folds that of *p*NPG$_4$ and ten-folds that of *p*NPG$_3$.

MO Functions and Stability of Molecule

Enzymatic reactions of S molecules, *p*NP-cellooligosaccharides (DP 1-5), caused by the β-glucosidase (E) that cleaves a cellulose into glucose units, are general acid catalytic hydrolysis induced by glutamic acid (Glu) (or aspartic

Table 2. Michaelis constant, specific activity, and physicochemical parameter of *p*NP-cellooligosaccharides and cellobiose by β-glucosidase.

(S)	K_m[a]	V_{max}[b]	SA[c]	logP	DM[d]	L_{TM}[e]	LM
*p*NPG$_1$[g]	1.33	65.6	164(−1.36)[i]	0.253	3.106	6.426	11.25
*p*NPG$_2$	1.60	0.14	0.90	−0.964	5.663	10.183	21.80
*p*NPG$_3$	0.32	0.25	7.50	−2.181	8.211	22.477	28.05
*p*NPG$_4$	0.02	0.63	11.20	−3.398	9.669	21.324	38.07
*p*NPG$_5$	0.01	2.63	22.50	−4.614	14.697	24.889	45.00
cellobiose[h]	0.24	6.00	ND	ND	ND	ND	ND

[a]mM, [b]mM min^{-1} mg^{-1}, [c]mM min^{-1} mg^{-1}, [d]dipole moment, [e]total length (Å) of substrate molecule, [f]lipole moment, [g,h]the values for V_{max} and SA are units min^{-1} mg^{-1}, [i]The extrapolated value in parenthesis was calculated according to the models (II) in Table 6. ND: not determined. The presented values for K_m and V_{max} were averages of triplicate experiments.

Table 3. Total energies, HOMO and LUMO energies (e.v.) of *p*NP-β-(glc)$_3$, (3), and their protonated forms (A–F) by the MOPAC-AMI calculation method.

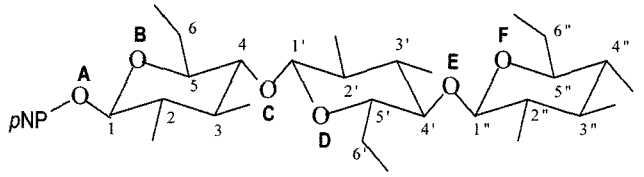

Type	HOMO	LUMO	$\Delta E_{HOMO-LUMO}$	Total E[h]	Stability
N[a]	-10.5696	-1.6003	-8.9693	41.635	1
A[b]	-12.0016	-5.9026	-6.0990	48.599	5
B[c]	-12.7590	-5.0569	-7.7021	53.727	7
C[d]	-12.6005	-3.9500	-8.6505	43.406	2
D[e]	-12.6006	-4.0359	-8.5647	45.489	3
E[f]	-12.0773	-4.9506	-7.1224	47.186	4
F[g]	-11.7218	-4.8491	-6.8727	50.085	6

1, Total energy=14.546 Kcal/mol, HOMO=-10.2910 e.v., LUMO=-1.4067 e.v.; 2, total energy=25.931 Kcal/mol, HOMO=-10.1888 e.v., LUMO=-1.2972 e.v. [a]Neutral molecule (3), [b-g]protonated form to the O_A[b], O_B[c], O_C[d], O_D[e], O_E[f], and O_F[g] atom, [h]1 electron volt (e.v.)=23.06 Kcal/mol.

acid; Asp) acting as the active site in E [2]. To understand the reaction route on an enzymatic acid hydrolysis reaction, total energy as well as LUMO and HOMO energies for oxonium ions, SH^+ (A–F) protonated to six oxygen atoms in the neutral compound 3 (N), were calculated with *p*NP-$(Glc)_3$ and summarized in Table 3. Because the stability of SH^+ was put in the order of (C)> (D)>(E)>(F), based on the energies protonated to oxygen atoms in the S molecule and the protonation reaction being done more easily in the order of -$(Glc)_1$-$(Glc)_2$->-$(Glc)_2$-$(Glc)_3$->*p*NP-$(Glc)_1$ unit, the (C) type of those SH^+ ions was the most stable compound. Therefore, the protonation reaction to the β-glycosidic bond would occur more in superiority than the protonation to the oxygen atom of the 1,5-ether linkage in the pyranose ring. In addition, the low energy difference ($\Delta E_{HOMO-LUMO}$) between LUMO and HOMO energies means that a linkage of an active site in a molecule is easily cleaved, whereas the cleavage is very difficult upon high energy value, and then these values are almost identical with the order of stability. Therefore, to investigate the carbon atom that was attacked by water molecule (H_2O) acting as a nucleophile according to the increase of positive charge after the protonation reaction (SH^+), the net charges of atoms including 3 (N) and SH^+ (A–F) ions were calculated and listed in Table 4. The anomeric carbon atom (C_1) in the protonation reaction will be a target of nucleophilic attack by H_2O in all cases, as the positive charge of C_1 is higher (C_1>C_4) than that of C_4. These results suggested that the exocyclic cleavage reactions by a kind of nucleophilic substitution reaction, in which first after protonation to SH^+ in the β-glycosidic bond, the cleavage of the C_1-O linkage was followed by making H_2O to attack the C_1 (C_1-O), occurred mainly rather than the endocyclic cleavages of making H_2O_2 to attack the C_1 of the protonated form (SH^+) to the oxygen atoms in the 1,5-ether linkage among the pyranose ring.

Interactions of Frontier Molecule Orbital

The MO diagram relating to FMO interactions [17] between the neutral molecule 3 (N) as S molecule, H_3O^+, SH^+ (C), which is the most stable compound among SH^+ compounds, and H_2O_2, using perturbation theory [18, 26], is shown in Fig. 1. The HOMO energy of the bond formation reaction between intermolecules is a scale of nucleophilicity where a molecule acts as a Lewis base, electron pair donor, whereas the LUMO energy is a scale of electrophilicity where a molecule acts as a Lewis acid, electron pair acceptor. The first step of the hydrolysis reaction is the formation of SH^+ by the protonation reaction of Glu (or Asp), which acts as the active site in the E molecule. Since the energy difference ($\Delta E_{HOMO-LUMO}$=-4.5271 e.v.) between the HOMO energy of neutral S molecule (N) and LUMO energy of H_3O^+ is smaller than the energy difference ($\Delta E_{LUMO-HOMO}$= -22.7468 e.v.) between the LUMO energy of S molecule 3 (N) and the HOMO energy of H_3O^+, an electrophilic reaction caused by a charge-controlled reaction pursuant to a strong Coulombic interaction between the HOMO energy of 3 (N)

Table 4. Net atomic charges of various constitutional atoms in *p*NP-β-(glc)$_3$, (3), and their protonated forms (A–F) by the MOPAC-AMI calculation method.

Type	β-(glc)$_1$				β-(glc)$_2$				β-(glc)$_3$		
	O_A	C_1	O_B	C_4	O_C	C_1	O_D	C_4	O_E	C_1	O_F
N[a]	-0.2207	0.1236	-0.2935	-0.0216	-0.2612	0.1433	-0.2512	0.0159	-0.2626	0.1731	-0.2831
A[b]	-0.0218	0.1434	-0.2758	0.0387	-0.2491	0.1131	-0.3039	-0.0132	-0.2567	0.1706	-0.2899
B[c]	-0.2436	0.1478	-0.0738	-0.0048	-0.2769	0.1683	-0.3077	-0.0242	-0.2366	0.1644	-0.3086
C[d]	-0.2547	0.1226	-0.2684	0.0464	-0.1467	0.1565	-0.2019	-0.0133	-0.2150	0.1609	-0.3238
D[e]	-0.2606	0.1194	-0.2636	-0.0464	-0.2311	0.0988	-0.1028	0.0094	-0.2828	0.1659	-0.3201
E[f]	-0.2479	0.1230	-0.2780	-0.0299	-0.2731	0.1188	-0.2488	-0.0201	-0.0568	0.1032	-0.2973
F[g]	-0.2572	0.1267	-0.2702	-0.0311	-0.2739	0.1371	-0.2505	-0.0192	-0.2266	0.0965	-0.1194

[a]Neutral molecule (3), [b-g]protonated form to the O_A[b], O_B[c], O_C[d], O_D[e], O_E[f], and O_F[g] atoms.

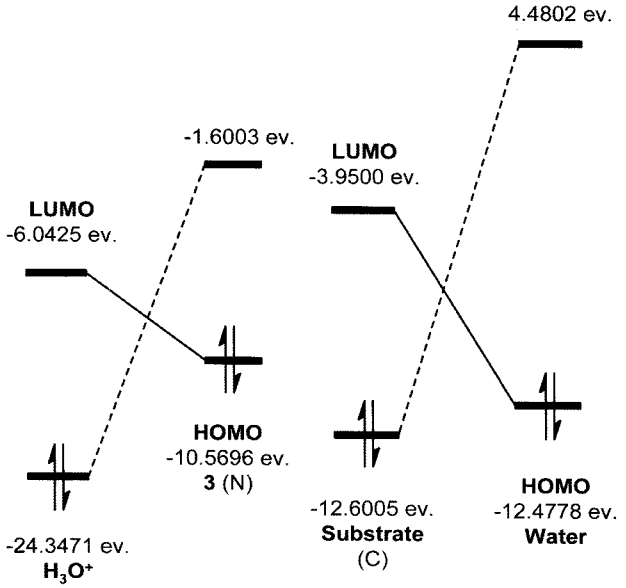

Fig. 1. FMO interaction between S molecule 3 (N: netural molecule; C: protonated form to the O_C atom, SH^+) and H_3O^+ (or water molecule) in the enzymatic hydrolysis of substrate 3, by the MOPAC (AMI) calculation method.

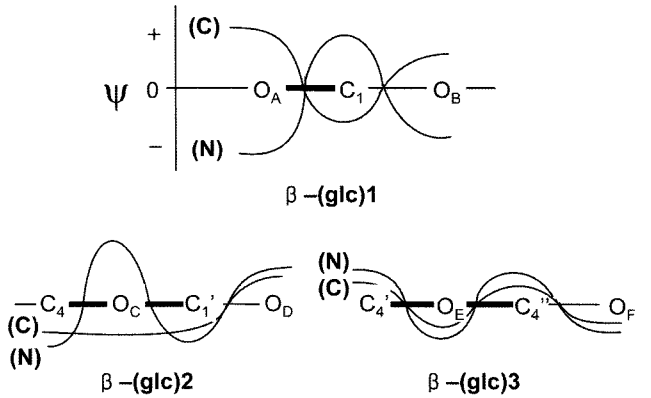

Fig. 2. Nodal properties based on AO coefficients (HOMO, 2pz) of the S molecule 3, by the MOPAC-AMI method.
N, Neutral molecule; C, protonated form to the O_C atom, SH^+; the bonds of bold parts indicate the β-1,4-glucosidic bond.

and the LUMO energy of H_3O^+ will occur more in superiority than a nucleophilic reaction by the orbital-controlled reaction between the LUMO energy of 3 (N) and the HOMO energy of H_3O^+. However, in the case of the reaction between SH^+ (C) and H_2O_2, since the energy difference ($\Delta E_{HOMO\text{-}LUMO}$= −17.0807 e.v.) between HOMO of SH^+ (C) and LUMO of H_2O_2 is larger than the energy difference ($\Delta E_{LUMO\text{-}HOMO}$= −8.5278 e.v.) between LUMO of SH^+ (C) and HOMO of H_2O_2, a nucleophilic reaction by the charge-controlled reaction pursuant to a strong interaction between the LUMO energy of SH^+ (C) and the HOMO energy of H_2O_2 would occur much faster.

AO Parameters and Cleavage Pattern

AO coefficients (2pz) of HOMO energy for various constitutional atoms were calculated in Table 5, and nodal properties based on AO coefficients are represented in Fig. 2, to investigate the cleavage pattern on the linkages of around the oxygen atoms in the oxonium ion SH^+ (A–F) and the S molecule 3 (N). From the apparent results, it would be expected that the cleavage possibility of those linkages is very high because of an existence of a node between C-O bonds in the N molecule. In particular, SH^+ (C), which is produced by protonation of the stable O_C atom, indicated that the cleavage does not occur in the second linkage of the β-1,4-(C_4-O_C-$C_{1'}$) glycosidic bond but in the $C_{1'}$-O_D bond. This corresponded well with the experimental results in Table 2. In case of each SH^+, which was produced by protonation reaction to one of six oxygen atoms in the S molecule 3 (N), the cleavage pattern of the C-O bond could be explained with the nodal properties based on AO coefficients as the following. First, in the O_A-C_1-O_B bond, N and B–F cleave totally all C-O bonds but A does not, it and in the C_4-O_C-C_1-O_D bond, N and A cleave all C-O bonds but B does not. C cleaves only the C_1-O_D bond, but D-F do only the C_4-O_c bond in contrast to C. In the case of the $C_{4''}$-O_E-$C_{1''}$-O_F bond, N and A-C cleave all C-O bonds, D cleaves the $C_{4''}$-O_E and $C_{1''}$-O_F bond, E does not cleave all the bonds, and F

Table 5. Atomic orbital (AO) coefficients (HOMO) of various constitutional atoms (2pz) in *p*NP-β-(glc)$_3$, (3), and their protonated forms (A–F) by the MOPAC-AMI calculation method.

Type	β-(glc)$_1$				β-(glc)$_2$				β-(glc)$_3$		
	O_A	C_1	O_B	C_4	O_C	C_1	O_D	C_4	O_E	C_1	O_F
N[a]	−0.1956	0.1883	−0.1056	−0.0451	0.0549	−0.0079	0.0148	0.0051	−0.0060	0.0034	−0.0032
A[b]	−0.0011	−0.0005	−0.0060	−0.0134	0.0189	−0.0200	0.0142	−0.0224	0.1453	−0.0301	0.0322
B[c]	−0.0006	0.0008	−0.0003	−0.0002	−0.0040	−0.0045	−0.0225	0.0284	−0.0652	0.0049	−0.0316
C[d]	0.2302	−0.0876	0.0345	−0.0024	−0.0018	−0.0016	0.0022	0.0008	−0.0006	0.0001	−0.0002
D[e]	−0.3577	0.0470	−0.0656	−0.0105	0.0172	0.0003	0.0002	−0.0016	0.0007	0.0004	−0.0001
E[f]	−0.2473	0.0714	−0.0921	−0.0041	0.0014	0.0006	0.0002	0.0001	0.0001	0.0001	0.0001
F[g]	−0.3648	0.0189	−0.0495	−0.0019	0.0001	0.0006	−0.0002	−0.0001	0.0001	0.0001	0.0001

[a]Neutral molecule (3), [b–g]protonated form to the O_A[b], O_B[c], O_C[d], O_D[e], O_E[f], and O_F[g] atoms.

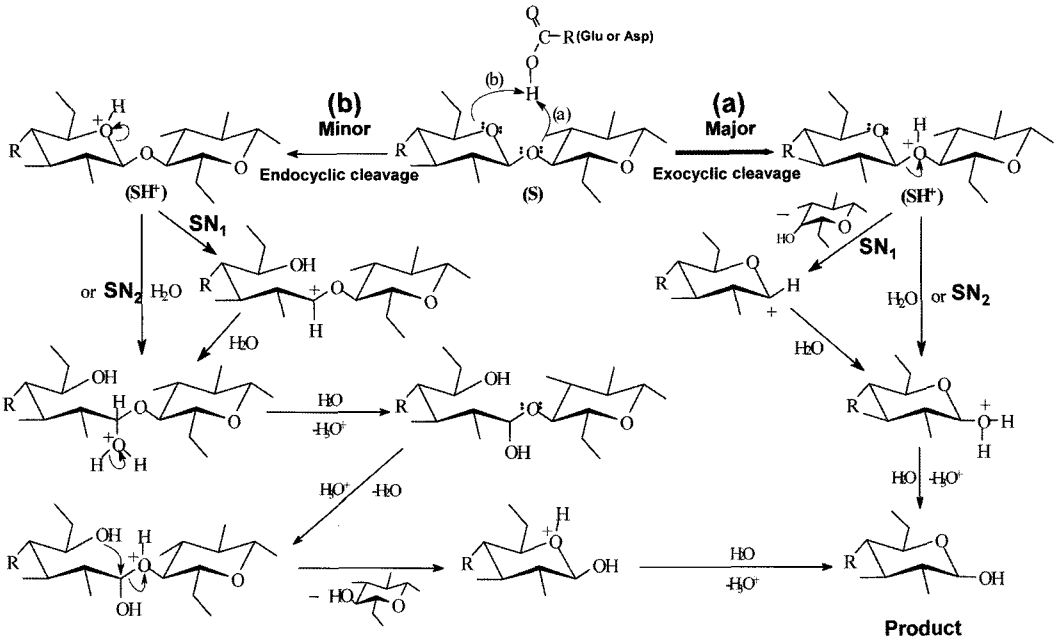

Scheme 1. Plausible enzymatic hydrolysis pathway of *p*NP-substrates by β-glucosidase from *C. uda* CS1-1. R=*p*-nitrophenoxy group.

cleaves only the C_4-O_E bond. These results suggest that the cleavage pattern of C-O bonds will be different according to verification of the position of an oxygen atom on which the protonation occurs. Experimentally, the cleavage pattern of β-glucosidase was similar to that of the endo-1,4-glucanase that cleaves cellulose to glucose units randomly, rather than the exo-1,4-glucanase from *C. uda* CS1-1 that cleaves cellobiose units [31], suggesting the exo-1,4-glucanase has uncompetitive inhibition reactivity.

Enzymatic Hydrolysis Reactions

The plausible pathway of the enzymatic acid-catalyst hydrolysis reaction between E and S molecules is proposed in Scheme 1, based on the MO functions and FMO interaction. In the step of the initiation reaction, E acts as a proton donor in general acid catalysis by Glu (or Asp) of the reaction site in the E receptor [3], whereas water molecules act as proton transfer agents, respectively.

The fast protonation reaction to the oxygen atom of the β-1,4-glycosidic bond occurs by H_3O^+ produced from the acidic catalysis reaction. The first step of the acidic hydrolysis reaction is the formation of SH^+, in which exocyclic cleavage by the electrophilic charge-controlled reaction occurs mainly, because the compound protonated to the oxygen atom of the β-1,4-glycosidic bond is more stable than that of the oxygen atom in the 1,5-ether linkage of the pyranose ring (Table 3). In addition, since endocyclic cleavage by the nucleophilic orbital-controlled reaction in which SH^+ is produced by protonation with H_3O^+ to the 1,5-ether linkage of pyranose occurs in the minority, the water molecules act as a nucleophile to the carbonium ion produced by the cleavage of the C-O bond in SH^+. The related previous research reported that all cellulolytic reactions including exocyclic (or endocyclic) cleavage is progressed by way of the carbonium ion [2]. Since both exocyclic and endocyclic cleavage reactions produce secondary carbonium ion, the reaction will be taken by competing with a unimolecular SN_1 reaction and a SN_2 reaction, which is a bimolecular nucleophilic substitution reaction to C_1 atom. Therefore, a series of the reaction progresses in that in the case of exocyclic cleavage, the C_1-O bond in the pyranose molecule is cleaved and thereafter the linkage is formed again, and in the case of endocyclic cleavage, the C_1-O bond of the β-1,4-glycosidic bond is cleaved.

Relationships Between Structure and Reactivity

QSARs are important tools to understanding the relationships between structure and reactivity of active compounds exhibiting certain biochemical activities. To investigate the QSAR on K_m and SA values obtained from the cellulolytic reaction between E and S, K_m, SA, and the physicochemical parameters of pNPG$_1$~pNPG$_5$ are listed in Table 2, in which the data relating to pNPG$_1$ values were not used because these values have no significant correlations with various kinds of the physicochemical parameters. The results showed that the more a number of glucose unit (β-(Glc) as a continuous chain) increases, the more the K_m value also increases. This means that it is easy to produce an E-S complex by increasing an affinity force between E and S, and the phenomenon was also identical for V_{max} and

Table 6. Statistical results of the best 2D-QSAR models with K_m, V_{max}, and specific activity of *p*NPG$_n$ (n=1–5).

Model	(I)	(II)	(III)
Values[a]	K_m	K_m	SA
n[b]	5 (n=1–5)	5 (n=1–5)	4 (n=2–5)
S[c]	1.781	2.008	245.26
F[d]	10.700	22.120	1250.03
r[e]	0.884	0.940	0.998
Intercept	1.412(±0.294)	2.130(±0.341)	−12.199(±0.680)
Weighting factor	logP: 0.35(±0.160)	L_{TM}: −0.086(±0.060)	DM:2.377(±0.160)

[a]Statistical values and weighting factors, [b]number of used compound, [c]means square, [d]F-value, [e]correlation coefficient.

SA. The 2D-QSAR models (I)–(III), which were induced to investigate the structure-activity relationships between E and S molecules, and those statistical parameters are summarized in Table 6. When the relationships on K_m value, MR (cm^3/mol), and logP constant [28] were examined, the weighting factor of the MR constant, which is a duplicate parameter that has correlations with both the steric factor and dispersion force, was very low. Because it is difficult to decide whether an interaction between the S molecule and β-glucosidase would be dependent on dispersion (MR>0) or steric (MR<0) effect [20], model (I) suggests that the K_m constant is dependent on logP, but the influence is minor. Moreover, as the correlations of length (L) and width (B_1) of the substituents in which the *p*NP parent was attached to the substituents, β-(Glc)$_1$–β-(Glc)$_5$, have been analyzed with K_m constant, respectively, only the length of the substituents did not have a significant correlation. Even though the effect is low, the total length (L_{MT}) of S molecules with *p*NP had a good correlation (r=0.940), as shown in model (II). The phenomenon could be explained with the reason that the L and B_1 of S molecules are flexible by various factors of the glucose units with *p*NP, and the *p*NP parent with its great hydrophobicity acts as an element to increase the affinity between the E and S molecules. As shown in Fig. 3, the SA of enzyme-like model (III) had a significant correlation for the DM of S molecules. These results suggest that the SA and K_m of β-glucosidase relating to cellulolytic reactivity would be influenced by the L_{MT} of the S molecule, including the DM and logP of S molecules.

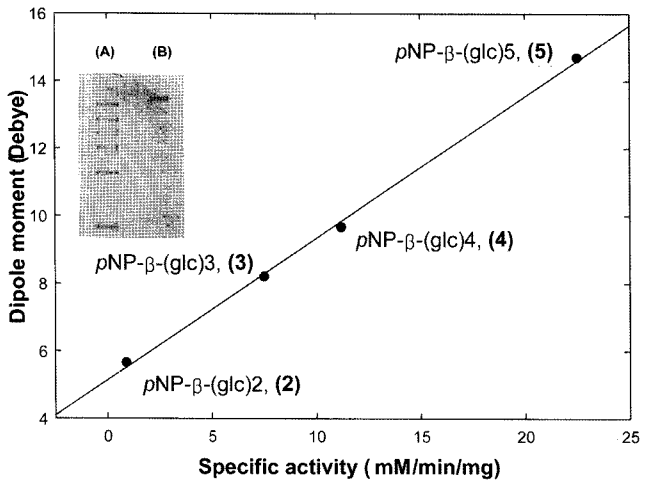

Fig. 3. Relationships between specific activities of β-glucosidase and dipole moment of the *p*NPG$_n$ (n=2–5) by model (III).
Inset **A**. Protein marker: β-Amylase (MW 200,000), Alcohol dehydrogenase (MW 150,000), Phosphorylase (MW 97,400), Bovine albumin (MW 66,000), Aldolase (MW 40,000), Carbonic anhydrase (MW 29,000), Cytochrome C (MW 12,000). Inset **B**. Molecular weight of the purified β-glucosidase.

Acknowledgments

This work was supported by a grant (No. R11-2002-100-03005) from the Excellent Research Center of Korea Science and Engineering Foundation, and by a Chungnam National University 2004 Research Grant.

References

1. Accelrys. 2000. TSAR: Proprietary software (Ver. 3.3), User Guide, Oxford Molecular: Solutions for Discovery Research. Oxford Molecular Ltd.
2. Baker, R. 1971. *Organic Chemistry of Biological Compounds: Foundations of Modern Biochemistry Series*, pp. 167–168. Prentice-Hall, Inc., Englewood Cliffs, New Jersy.
3. Bender, M. L., R. J. Bergeron, and M. Komiyama. 1984. General acid-base catalysis: Enzymatic reactions, pp. 116–129. The Bioorganic Chemistry of Enzymatic Catalysis. John Wiley & Sons, New York.
4. Chen, H. G., X. Yan, X. Y. Liu, M. D. Wang, H. M. Huang, X. C. Jia, and J. A. Wang. 2006. Purification and characterization of novel bifunctional xylanase, XynIII, isolated from *Aspergillus niger* A-25. *J. Microbiol. Biotechnol.* **16:** 1132–1138.
5. Cornish-Bowden, A. 1995. *Fundamentals of Enzyme Kinetics*, pp. 343–348. Revised Edition. Portland Press.
6. Devillers, J. and A. T. Balaban. 1999. *Topological Indices and Related Descriptors in QSAR and QSPR*, pp. 1–20. Gordon and Breach Science Publishers, Switzerland.
7. Dewar, M. J. S., E. G. Zoebish, E. F. Healy, and J. J. P. Stewart. 1985. AMI: A new general purpose quantum

mechanical molecular model. *J. Am. Chem. Soc.* **107:** 3902–3909.
8. Fleming, I. 1976. *Frontier Orbitals and Organic Chemical Reactions*, pp. 34–85. John Wiely & Sons, London.
9. Gupta, S. P. 1987. QSAR studies on enzyme inhibitors. *Chem. Rev.* **87:** 1183–1253.
10. Hansch, C., E. W. Deutsch, and R. N. Smith. 1965. The use of substituent constants and regression analysis in the study of enzymatic reaction mechanism. *J. Am. Chem. Soc.* **87:** 2738–2742.
11. Hansch, C. and K. N. von Kaulla. 1970. Fibrinolytic congeners of benzoic acid and salicylic acid: A mathematical analysis of correlation between structure and activity. *Biochem. Pharmacol.* **19:** 2193–2200.
12. Hansch, C. and K. N. von Kaulla. 1975. *Synthetic Fibrinolytic Thrombix Agents, Chemical, Biochemical, Pharmocological and Clinical Aspects*, pp. 227–279. Charles, C. Thomas, Springerfield, III.
13. Hansch, C. and A. Leo. 1995. *Exploring QSAR: Fundamentals and Applications in Chemistry and Biology*, pp. 223–288. ACS Professional Reference Book, American Chemical Society, Washington, DC.
14. Hoh, Y. K., H. H. Yeoh, and T. K. Tan. 1992. Properties of β-glucosidase purified from *Aspergillus niger* mutant USDB0827 and USDB0820. *Appl. Microbiol. Biotechnol.* **37:** 590–593.
15. Jin, J. H., U. S. Jung, J. W. Nam, Y. H. In, S. Y. Lee, D. H. Lee, and J. W. Lee. 2005. Construction of comprehensive metabolic network for glycolysis with regulation mechanisms and effectors. *J. Microbiol. Biotechnol.* **15:** 161–174.
16. Joshi, M. D., G. Sidhu, I. Pot, G. D. Brayer, S. G. Withers, and L. P. Mclntosh. 2000. Hydrogen bonding and catalysis: A novel explanation for how a single amino acid substitution can change the pH optimum of a glycosidase. *J. Mol. Biol.* **299:** 255–279.
17. Klopman, G. 1974. *Chemical Reactivity and Reaction Paths*, pp. 55–165. John Wiely & Sons, New York.
18. Kubinyi, H. 1993. *QSAR: Hansch Analysis and Related Approaches*, pp. 27–85. VCH Publishers, New York, NY.
19. Laemmli, U. K. 1970. Cleavage of structural proteins during the assembly of the head of bacteriophage T4. *Nature* **227:** 680–685.
20. Li, W. and I. Kubo. 2004. QSAR and kinetics of the inhibition of benzaldehyde derivatives against *Sacrophaga neobelliaria* phenoloxidase. *Bioorg. Med. Chem.* **12:** 701–713.
21. Lowry, O. H., N. J. Rosebrough, A. L. Farr, and R. J. Randall. 1951. Protein measurement with the Folin phenol reagent. *J. Biol. Chem.* **193:** 265–275.
22. Oleson, E. C. and R. E. Christofferson. 1979. *Computer-assisted Drug Design*, pp. 161–189. Acs. Symp. Ser. No. 112, ACS, Washington, D.C.
23. Porter, W. R. and W. F. Trager. 1977. Improved non-parametric statistical methods for the estimation of Michaelis-Menten kinetic parameters by direct linear plot. *Biochem. J.* **161:** 293–302.
24. Raabo, E. and T. C. Terkildsen. 1960. On the enzymatic determination of blood glucose. *Scand. J. Clin. Lab. Invest.* **12:** 402–407.
25. Seidle, H. F., I. Marten, O. Shoseyov, and R. E. Huber. 2004. Physical and kinetic properties of the Family 3 β-glucosidase from *Aspergillus niger* which is important for cellulose breakdown. *Protein J.* **23:** 11–23.
26. Seo, D. K., G. Papoian, and R. Hoffmann. 2000. Generalized perturbational molecular orbital (PMO) theory. *Int. J. Quant. Chem.* **77:** 408–420.
27. Stewart, J. J. 1990. MOPAC: A semiempirical molecular orbital program. *J. Comp. Aided Mol. Design* **4:** 1–105.
28. Taylor, P. J. 1990. In Hydrophobic properties of drug,, pp. 241–294. *In* C. Hansch, P. G. Sammes, and J. B. Taylor (eds.). *Comprehensive Medical Chemistry.* Pergamon Press, Toronto.
29. Torronen, A. and J. Rouvinen. 1997. Structural and functional properties of low molecular weight endo-1,4-beta-xylanase. *J. Biotechnol.* **57:** 137–149.
30. Verloop, A. W., W. Hoogenstraten, and J. Tipker. 1976. Development and application of new steric substituent parameters in drug design, Vol. 7, pp. 165–207. *In* E. J. Ariens (ed.). *Drug Design.* Academic Press, New York.
31. Yoon, M. H. and W. Y. Choi. 2007. Characterization and action patterns of two β-1,4-glucanases purified from *Cellulomonas uda* CS1-1. *J. Microbiol. Biotechnol.* In Press.